J Physiol 587.6 (2009) pp 1265–1281

The Journal of Physiology

Activity-dependent depression of the spike after-depolarization generates long-lasting intrinsic plasticity in hippocampal CA3 pyramidal neurons

Jon T. Brown and Andrew D. Randall

MRC Centre for Synaptic Plasticity, Department of Anatomy, University of Bristol, University Walk, Bristol BS8 1TD, UK

Persistent plastic changes to the intrinsic excitability of neurons have substantial implications for computational processing within the CNS. We have identified and characterized a novel long-lasting form of intrinsic plasticity in hippocampal CA3 pyramidal cells. Although the patterns of action potential firing elicited in this cell population by depolarizing current injections exhibited considerable diversity, practically all cells produced an initial high frequency (>100 Hz) burst of two to five spikes. This burst involved conductances that were responsible for the prominent spike afterdepolarization of CA3 pyramids. Long-lasting changes in the firing behaviour of CA3 cells were produced by conditioning stimuli (CS) consisting of either periods of depolarization in voltage clamp or periods of short (2 or 4 spikes) high frequency (circa 100 Hz) burst firing at 5 or 10 Hz. CS-induced changes included substantial prolongation of the first inter-spike interval and increased spike jitter. Similar CS-induced changes were seen when the test stimulus used to elicit firing resembled a glutamatergic EPSC. In line with this, a long-lasting depression of the ADP was elicited by the same CS that altered firing patterns of CA3 cells. Conditioning-induced changes in both spiking patterns and ADP amplitude were blocked by buffering intracellular Ca^{2+} with BAPTA. Furthermore, the Kv7 channel blocker XE991, a cognitive enhancer, both enhanced the ADP and completely eliminated its conditioning-induced depression. These findings indicate that a persistent enhancement of Kv7 channels, following a transient increase in cytoplasmic Ca^{2+}, results in a prolonged depression of the ADP in CA3 pyramidal neurones.

(Received 25 November 2008; accepted after revision 22 January 2009; first published online 2 February 2009)
Corresponding author J. Brown: MRC Centre for Synaptic Plasticity, Department of Anatomy, University of Bristol, University Walk, Bristol BS8 1TD, UK. Email: jon.brown@bristol.ac.uk

Intrinsic plasticity is a form of neuronal plasticity that concerns CS-induced changes to core membrane properties of neurons that in turn affect their subsequent electrical responsiveness. Like synaptic plasticity, with which it is often closely entwined, intrinsic plasticity occurs in many forms covering a time scale from a few milliseconds to hours and very likely much longer. Intrinsic plasticity can be induced by the cell's own patterns of electrical activity (Egorov *et al.* 2002) or can arise from external influences including synaptic activity (Aizenman & Linden, 2000; Mellor *et al.* 2002; Sourdet *et al.* 2003; Fan *et al.* 2005; Xu *et al.* 2005). Furthermore, plastic changes to intrinsic neuronal properties can also arise as a consequence of a pathological environment (Chen *et al.* 2001; Wellmer *et al.* 2002). There is a growing understanding that long lasting changes in intrinsic neuronal excitability have the potential to play key roles in experience-dependent learning and memory (Disterhoft *et al.* 1986; Coulter *et al.* 1989; Moyer *et al.* 1996; McEchron *et al.* 2001; Zhang & Linden, 2003).

Spike after-potentials, i.e. after-hyperpolarizations (AHPs) and after-depolarizations (ADPs), play an important role in shaping neuronal firing patterns (Storm, 1987; Williams & Stuart, 1999; Yue & Yaari, 2004; Gu *et al.* 2005; Bean, 2007). The mechanisms and functions of the ADP in hippocampal pyramidal neurons have received growing attention in recent years (Yue & Yaari, 2004; Metz *et al.* 2005; Yue *et al.* 2005; Vervaeke *et al.* 2006; Kaczorowski *et al.* 2007; Metz *et al.* 2007; Chen & Yaari, 2008). One membrane conductance that appears to play an important role in the regulation of the ADP is that mediated by Kv7/KCNQ/M-channels (known hereafter as Kv7 channels) (Yue & Yaari, 2004; Vervaeke *et al.* 2006; Yue & Yaari, 2006). Kv7 channels are thought to underlie the neuronal M current (I_M) (Wang *et al.* 1998), a slowly activating, non-inactivating K^+ conductance which

DOI: 10.1113/jphysiol.2008.167007

is often active at membrane potentials around those observed in resting CNS neurons (Brown & Adams, 1980). Blockade of Kv7 channels enhances the ADP, whereas enhancing activation gating of Kv7 channels suppresses the ADP, resulting in corresponding changes to neuronal firing behaviour (Yue & Yaari, 2004; Vervaeke *et al.* 2006).

Despite their important role controlling neuronal output, there are surprisingly few reports of persistent plastic changes to spike after-potentials. Both pharmacological and synaptic activation of group I metabotropic glutamate receptors (Sourdet *et al.* 2003; Ireland *et al.* 2004) and kainate receptors (Melyan *et al.* 2002, 2004) can induce long term modulation of AHPs. Recently, a millisecond scale enhancement of the ADP that arises from acute Ca^{2+}-depedent inhibition Kv7 channels has been described in CA1 pyramidal cells (Chen & Yaari, 2008). To date, however, there have been no reports of long-term plastic changes to the ADP, and associated persistent alterations to neuronal firing and output.

In this study we describe how CA3 neuron firing patterns can undergo a radical and long-lasting reconfiguration in response to conditioning stimuli that are pertinent to both the physiological and patho-physiological activity of these cells. This novel, persistent form of intrinsic plasticity results in changes to spike frequency, attenuation and jitter. This change is associated with, and arises from, a lasting depression of the ADP. This modification of the ADP is entirely dependent on the presence of functional Kv7 channels, suggesting that I_M plays a previously unreported and pivotal role in long-term neuronal plasticity.

Methods

Slice preparation and electrophysiology

All procedures were carried out in accordance with UK Home Office guidelines set out in the Animals (Scientific Procedures) Act 1986. Male Wistar rats aged between 2 and 3 weeks were killed by cervical dislocation. Following decapitation and isolation of the brain, horizontal hippocampal slices of 300 μm thickness were prepared using a Leica VT1200 as described previously (Brown & Randall, 2005). Following their isolation, slices were transferred to an submerged recording chamber maintained at $32 \pm 1^{\circ}$C, perfused ($\sim$2–3 ml min^{-1}) with an artificial cerebrospinal fluid (aCSF) comprising (mM): NaCl, 124; KCl, 3; $NaHCO_3$, 26; $CaCl_2$, 2; NaH_2PO_4, 1.25; $MgSO_4$, 1; D-glucose, 10; equilibrated with 95% O_2 and 5% CO_2. This aCSF was additionally supplemented with 1,2,3,4-tetrahydro-6-nitro-2,3-dioxo-benzo[f]quinoxaline-7-sulfonamide (NBQX; 5 μM), L-689,560 (5 μM) and either gabazine (10 μM) or picrotoxin (50 μM) to block AMPA/kainate, NMDA and $GABA_A$ receptors, respectively. Whole cell patch clamp recordings were made using borosilicate glass microelectrodes (3–5 MΩ) containing (mM): potassium gluconate, 130; KCl, 20; K-Hepes, 10; EGTA, 0.2; Na-GTP, 0.3; Mg-ATP, 4; pH 7.3, 285–290 mosmol l^{-1}. A similar potassium gluconate-based internal solution has been shown to result in very stable recordings of the ADP in hippocampal neurons (Kaczorowski *et al.* 2007). In some experiments 10 mM BAPTA was added to the internal solution to more strongly buffer cytoplasmic Ca^{2+}. The pairing of our aCSF and electrode solution produced a liquid junction potential of 13 mV, which was corrected for arithmetically. Current clamp recordings were made using the bridge circuit of a MultiClamp 700B amplifier (Molecular Devices, Union City, CA, USA). Only cells with a junction potential-corrected resting membrane potential more negative than -60 mV were used for experiments. Since the ADP amplitude was voltage dependent (Fig. 1*D*), in most experiments somatic current injection, using the automatic slow current injection function of the MultiClamp 700B amplifier (5 s time constant), was used to keep the pre-stimulus membrane potential at a set level. The membrane potential chosen was usually the neuron's initial resting potential. When studying the ADP, however, the pre-stimulus membrane potential was, when required, slightly hyperpolarized (by $\leq$ 5mV) to prevent the ADP from firing any secondary action potentials (see Fig. 1*F* for an example of how this is achieved).

Mock synaptic potentials were induced using current injection waveforms that approximated glutamatergic EPSCs. These were generated from the sum of a rising and decaying exponential function:

$$y = e^{-x/\tau_{\text{decay}}} - e^{-x/\tau_{\text{rise}}}$$

where τ_{decay} was the rate constant of decay of the mock synaptic event and τ_{rise} the rate constant of the rising phase. In all cases $\tau_{\text{rise}} = 0.3$ ms, whilst τ_{decay} was varied to alter the duration of the mock synaptic event. The peak of the resultant curve was then appropriately scaled to generate a current waveform capable of firing action potentials. Data were filtered at 6 kHz and digitized at 20 kHz (or filtered at 10 kHz and digitized at 50 kHz for spike measurements) and recorded to a personal computer using Clampex 10 software (Molecular Devices).

Drugs

NBQX and gabazine were purchased from Ascent Scientific (Weston-super-Mare, UK). L-689,560, ZD7288, retigabine and XE991 were purchased from Tocris-Cookson (Bristol, UK). Picrotoxin was purchased from Sigma-Aldrich (Poole, UK). All drugs were applied to the slice via the perfusion system.

Data analysis

ADP amplitude and spike analyses were performed using Clampfit 10 software (Molecular Devices); additional data processing was carried out using Microsoft Excel. It must be noted that obtaining a measure of the true magnitude of the ADP presents technical issues. This is because it rides atop the voltage trajectory of the membrane potential discharge that occurs after current injection has ceased. It is therefore difficult to isolate the ADP from the trajectory of membrane discharge because the rate of the latter is a function of the instantaneous membrane conductance, and thus subtracting a scaled subthreshold membrane potential discharge curve, for example, is not a feasible option. Consequently, for the purposes of this paper we, like others who study the ADP, have simply measured the peak of the ADP above the pre-stimulus (i.e. current injection) baseline membrane potential (see Fig. 1*B*). Much of this amplitude (we estimate typically 60–70%) does not arise from the ADP but reflects residual charge held within the membrane capacitance following the prior current injection. Consequently, what appears as a 20% change in this measure of the ADP is likely to represent a 50% or greater change in the true underlying ADP amplitude.

Input resistance was determined using Ohm's law applied to the voltage deflection in response to a 500 ms injections of 50 pA of hyperpolarizing current applied at the resting potential. From the same voltage responses the membrane time constant was determined from a single exponential fit to the membrane charging curve. The extrapolated input resistance was determined with Ohm's law from an infinite time extrapolation of this fit. The extrapolated input resistance reflects resting input resistance prior to the additional activation of I_h that occurs upon hyperpolarization. Action potential threshold was measured as the voltage where the first derivative of the spike waveform exceeds 10 V s^{-1} (Naundorf *et al.* 2006). Spike jitter was calculated as the standard deviation of the first inter-spike interval in the 5 min prior to a conditioning stimulus and an identical number of points 25–30 min after the conditioning stimulus.

Table 1. Electrophysiological properties of CA3 neurons

Resting membrane potential	-75 ± 1 mV
Membrane time constant (*)	48.4 ± 1.3 ms
Input resistance (*)	167 ± 4 MΩ
Extrapolated input resistance (*)	204 ± 5 MΩ
% sag (*)	17.3 ± 1.1%
Mean number of action potentials (current injection: 300/200 pA)	$10.4 \pm 0.5/8.0 \pm 0.5$
Action potential threshold†	-58.1 ± 0.3 mV
Action potential peak†	29.0 ± 0.5 mV
Action potential width at 0 mV†	0.57 ± 0.01 ms
ADP amplitude‡	15.2 ± 0.5 mV
n	95

*Calculated from the voltage deflection in response to a −100 pA current injection. †Measured from first spike in response to a +300 pA depolarizing current injection. ‡ADP measured following a single action potential elicited by a 2 ms, +2 nA depolarizing current injection.

Results

High frequency burst firing in CA3 cells driven by an ADP

Many neocortical pyramidal neurons are known to fire action potentials in high frequency bursts, a pattern of activity that is widely thought to be important for cell signalling and neuronal plasticity (Kandel & Spencer, 1961; Jarsky *et al.* 2008). Consequently, using whole cell current clamp recordings, we first sought to carefully establish the basal membrane properties and stimulus-driven firing patterns present within the CA3 pyramidal neuron population. The basic membrane properties of the CA3 neurons are summarized in Table 1. The response of CA3 pyramids to depolarizing current injections exhibited considerable cell-to-cell variability. To illustrate this, Fig. 1*A* presents voltage responses to 500 ms duration −100 pA (hyperpolarizing) and +200 pA (depolarizing) current injections applied to three individual CA3 cells at resting potential. These examples represent the three broad patterns of activity we have observed in hundreds of similar recordings. There are cells that fired only an initial short 'burst' of two to four action potentials before entirely ceasing to fire (top), 'tonically firing' cells that generated an initial burst followed by regular action potentials throughout the depolarizing stimulus (bottom) and cells with an intermediate firing phenotype consisting of an initial burst and a period of low frequency firing that terminated during the stimulus (middle). Although depolarization-induced firing patterns are quite diverse across the CA3 cell population, there is invariably a very high frequency burst of action potentials initiated towards the start of a period of depolarization (Fig. 1*B*).

We were interested to establish what produced the initial high frequency burst of action potentials in CA3 pyramidal cells exposed to a depolarizing stimulus. In CA1 pyramidal neurons, the conductances that underpin the ADP are reported to be pivotal for generating high frequency burst firing (Metz *et al.* 2005, 2007; Yue *et al.* 2005; Yue & Yaari, 2006). To elicit an ADP a very brief (2 ms) strong (2 nA) depolarizing current injection was used (Fig. 1*C*). This stimulus always rapidly generates at least one action potential in CA3 pyramidal cells. Furthermore, the current injection stimulus is stopped

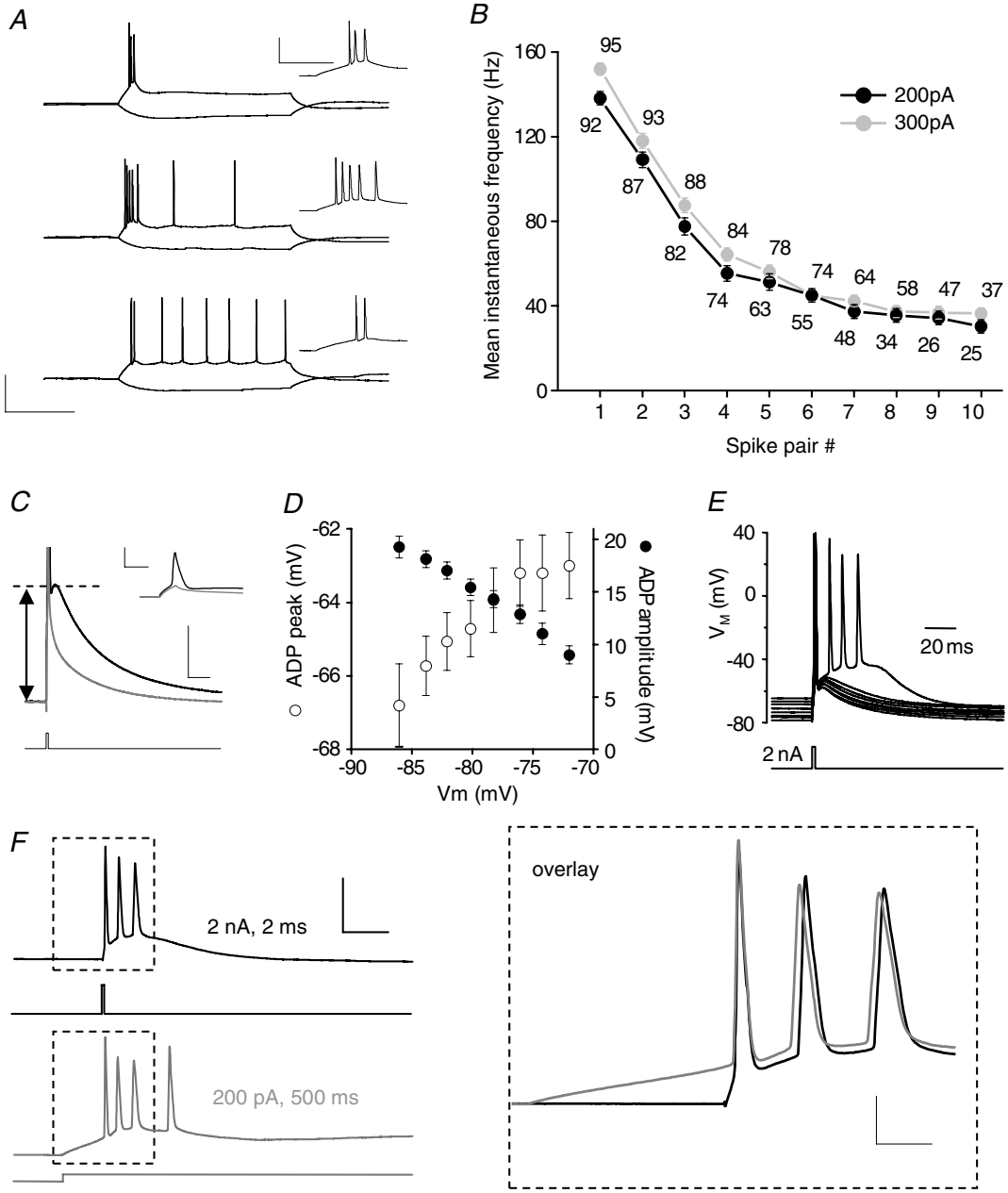

Figure 1. Burst firing in CA3 neurons is driven by an ADP
A, traces from current clamp recordings of 3 CA3 pyramidal neurons at resting potential showing the response to 500 ms hyperpolarizing and depolarizing current injections (−100, +200 pA, respectively). The neurons exhibit varying degrees of spike frequency accommodation. Calibration: 200 ms, 50 mV. Inset traces show the initial portion of the voltage deflection, illustrating that the first 2–5 action potentials occur in a high frequency burst. Calibration: 50 ms, 50 mV. *B*, plot of the mean instantaneous firing frequency of the first 10 action potential pairs for the cells depicted in *B* using a 200 and 300 pA depolarizing current injection. Number of cells included for each data point is noted on the graph. *C*, a current clamp recording from a CA3 pyramidal neuron illustrating the response to a brief, large (2 ms, 2 nA) somatic current injection which results in a single action potential followed by an after depolarization (ADP) superimposed on a slow membrane potential discharge. Calibration: 20 ms, 10 mV (main trace); 3 ms, 50 mV (inset trace). Bath application of tetrodotoxin (TTX; 1 μM) inhibited the Na^+ channel-dependent action potential (inset; grey trace). This revealed a slow discharge of the membrane potential which is distinct from the ADP. The arrow indicates amplitude of the ADP relative to the baseline membrane potential. In the main trace, the action potential is truncated for clarity. *D*, varying the somatic membrane potential by injecting different amounts of constant current altered the amplitude and the peak membrane potential attained by the ADP ($n = 6$–12). At more depolarized pre-stimulus potentials the resultant ADP was smaller but still reached a more depolarized peak. Pre-stimulus membrane potentials less negative than −70 mV often resulted in the ADP

at, or just prior to, the peak of the spike. Immediately following the fast repolarization phase of action potentials elicited in this manner, a prominent ADP was always observed riding atop the trajectory of membrane potential discharge. The amplitude of the ADP was dependent on the membrane potential; thus when elicited from more depolarized pre-stimulus membrane potentials the ADP was smaller (Fig. 1*D*, filled symbols). It should be noted, however, that, due to the relatively shallow slope of this relationship, the ADP peaks at more depolarized levels when generated from a more depolarized pre-stimulus potential (Fig. 1*D*, open symbols).

As reported for other pyramidal cells, given either a sufficiently large ADP or a suitably depolarized resting potential, the ADP was able to drive one or more additional action potentials to fire after the current injection had been terminated (Fig. 1*E* and *F*). At resting potential this was the case in a proportion of the CA3 cells we studied (Fig. 1*F*). The high frequency burst of spikes driven by an ADP and the burst that occurs during the first ∼50 ms of longer depolarizing current injections have very similar properties. This can be illustrated by overlaying these two types of burst recorded from a single cell (Fig. 1*F*). Bursts of spikes with a similar profile can be observed using non-invasive extracellular recordings of antidromic activation of CA3 pyramids (A. D. Randall, unpublished observations). This indicates that the bursting properties of CA3 pyramids described here are not an experimental artefact produced by whole cell patch clamp recording methods.

Long term alteration to burst firing properties induced by depolarization

In the absence of any intervention, the firing pattern of any given CA3 cell in response to regular current injections at 0.05 Hz was very consistent from sweep to sweep. We discovered, however, that a conditioning stimulus consisting of a period of tonic depolarization applied in voltage clamp ($V_{\mathrm{hold}} = -14$ mV for 150 s) could induce a long-lasting reconfiguration of firing measured when the cells were returned to current clamp and again stimulated with identical depolarizing current injections. Figure 2*A* presents examples of the responses to a 200 pA current injection in a typical CA3 pyramidal cell before and 30 min after such a conditioning stimulus. It was immediately apparent that this conditioning protocol produced a dramatic long-lasting change in the firing pattern of the cell, in particular the initial high frequency burst of action potentials was clearly modified such that the interval between the first two spikes was substantially prolonged post-conditioning.

Figure 2*A* illustrates the time course of this conditioning-induced change in the first interspike interval (ISI) pooled from 14 identical experiments. Additional analysis of the interval between all spikes elicited by current injection before and after application of the depolarizing conditioning stimulus revealed a complete elimination of high frequency firing post-conditioning, although the ability to fire spikes at gamma band frequencies (∼40–50 Hz) remained intact (Fig. 2*C*). Importantly these changes were not associated with a significant changes in input resistance, membrane time constant or holding current employed to keep the cell at the set pre-stimulus resting potential (Fig. 2*B*).

Spike-timing reliability is thought to play an important role in certain forms of synaptic plasticity (Dan & Poo, 2006) and neuronal network activity (Foffani *et al.* 2007). Prior to conditioning, the first few action potentials elicited by repeatedly applied depolarizing current injections to CA3 cells exhibited high fidelity spike timing (Fig. 2*D*). Post-conditioning, the increase in the first interspike interval was associated with a clear decrease in fidelity of spike timing. This is illustrated for an example cell in the spike raster plot shown in Fig. 2*D*. To quantify spike-timing reliability we calculated jitter for the first ISI. Prior to the conditioning stimulus this averaged 1.58 ± 0.29 ms ($n = 16$). Following the depolarizing conditioning stimulus, the first ISI jitter was significantly increased and remained greater for at least 30 min (2.80 ± 0.44 ms; $P < 0.01$, $n = 16$; Fig. 2*D*). Taking the findings presented in Fig. 2 together, a major outcome of inducing this form of intrinsic plasticity in CA3 cells is elimination of the ability to fire tightly timed high frequency spike bursts in response to depolarizing stimuli.

Long term depression of the ADP induced by depolarization

As discussed above, high frequency burst firing of hippocampal pyramids is driven by the same conductances that produce the spike after-depolarization

driving additional spikes in a substantial proportion of cells. *E*, an example recording illustrating that at sufficiently depolarized membrane potentials (although still within the range of V_{rest}), the ADP reached firing threshold and triggered a burst of a further 3 spikes. *F*, a burst of spikes triggered by a suprathreshold ADP compared to the burst of spikes associated with a more prolonged depolarizing stimulus recorded from the same cell. The traces are aligned to the peak of the first action potential. The regions in the boxes are overlaid and shown on an expanded time scale on the right. Note the near identical pattern of high frequency activity induced by the ADP-driven burst. Calibration: 20 ms, 50 mV. Inset: 5 ms, 20 mV.

(Yue & Yaari, 2004; Yue *et al.* 2005; Spruston & McBain, 2007). Consequently, we hypothesized that a conditioning-induced, long-term modification to an ADP could underlie aspects of modifications to firing patterns observed in CA3 neurons following application of an appropriate conditioning stimulus. When evoked every 20 s, the amplitude of the ADP was very stable with respect to time. A long-lasting depression of the ADP, however, could be consistently induced by the same conditioning protocol used to elicit the persistent plastic change in the experiments shown in Fig. 2 (i.e. voltage clamp at −14 mV for 150 s). Thus, prior to conditioning, the ADP amplitude was 14.1 ± 1.0 mV, whereas 30 min post-conditioning, the ADP amplitude was 11.3 ± 0.9 mV, a significant reduction of 20.3 ± 3.3% ($P < 0.01$; $n = 13$; Fig. 3*A* and *B*). Reducing the duration of the depolarizing conditioning stimulus by a half log unit (to 48 s) resulted in a significant, but lesser, long-lasting depression of the ADP (control ADP amplitude, 15.0 ± 1.1 mV; ADP amplitude 30 min post-depolarization, 13.3 ± 0.9 mV; $P < 0.05$, $n = 13$;

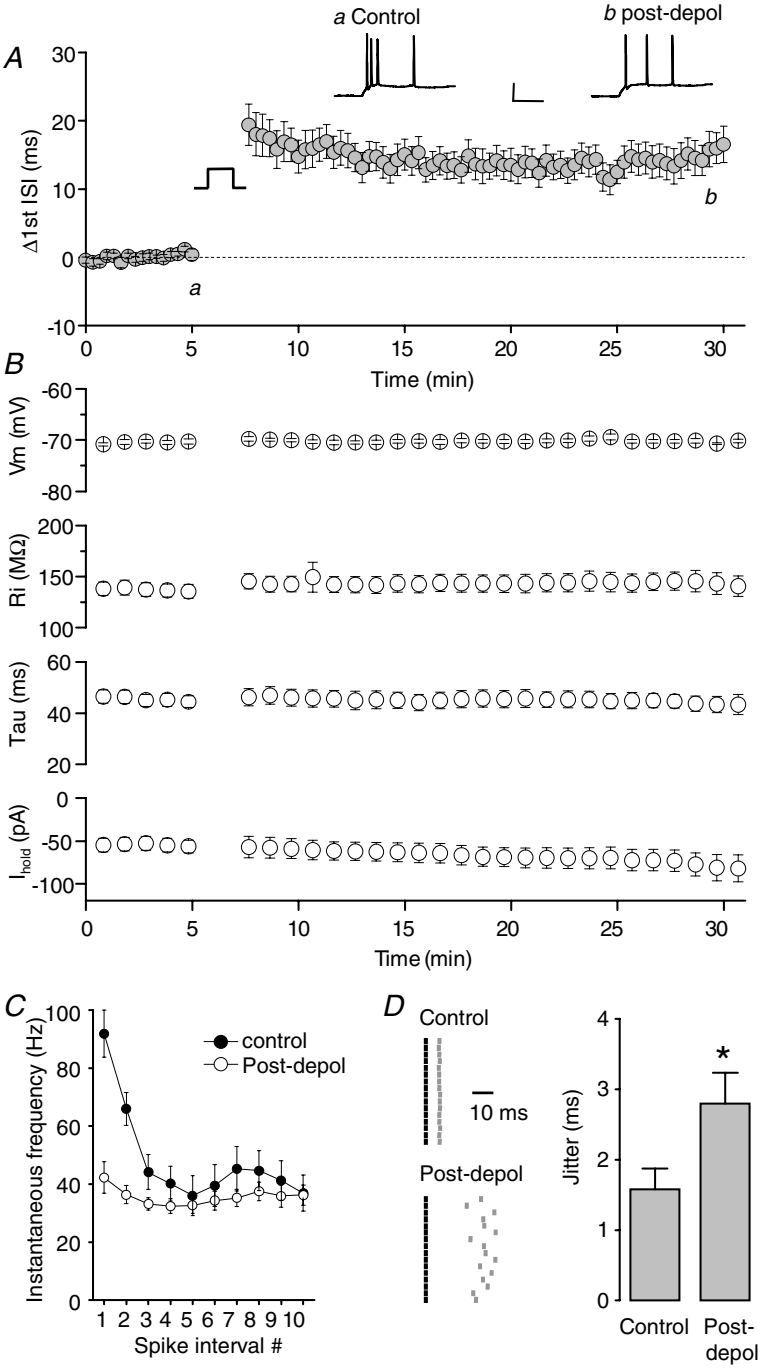

Figure 2. Transient depolarization results in loss of high frequency firing
A, pooled time courses illustrating the change in first ISI in 16 CA3 pyramidal neurons. Intrinsic plasticity was induced using a 150 s depolarization from −84 to −14 mV. Example recordings from a CA3 neuron taken immediately before (*a*) and 30 min after (*b*) the depolarizing conditioning stimulus. Calibration: 50 ms, 30 mV. *B*, summary data illustrating the membrane potential (which was kept constant by a slow current injection), input resistance, membrane time constant and current required to maintain the cell at a set membrane potential. None of these parameters significantly changed following the depolarizing stimulus. *C*, spike frequency accommodation was largely abolished post conditioning. *D*, consecutive raster plots showing the first ISI induced by a 200 pA depolarization immediately before and 30 min after the conditioning stimulus was applied. The first spikes are represented by the black lines, the second spikes by the grey lines. The timing of the second spike is shown relative to the first spike. Pooled data show significant increase in first ISI jitter following the induction of intrinsic plasticity (*$P < 0.01$, $n = 16$).

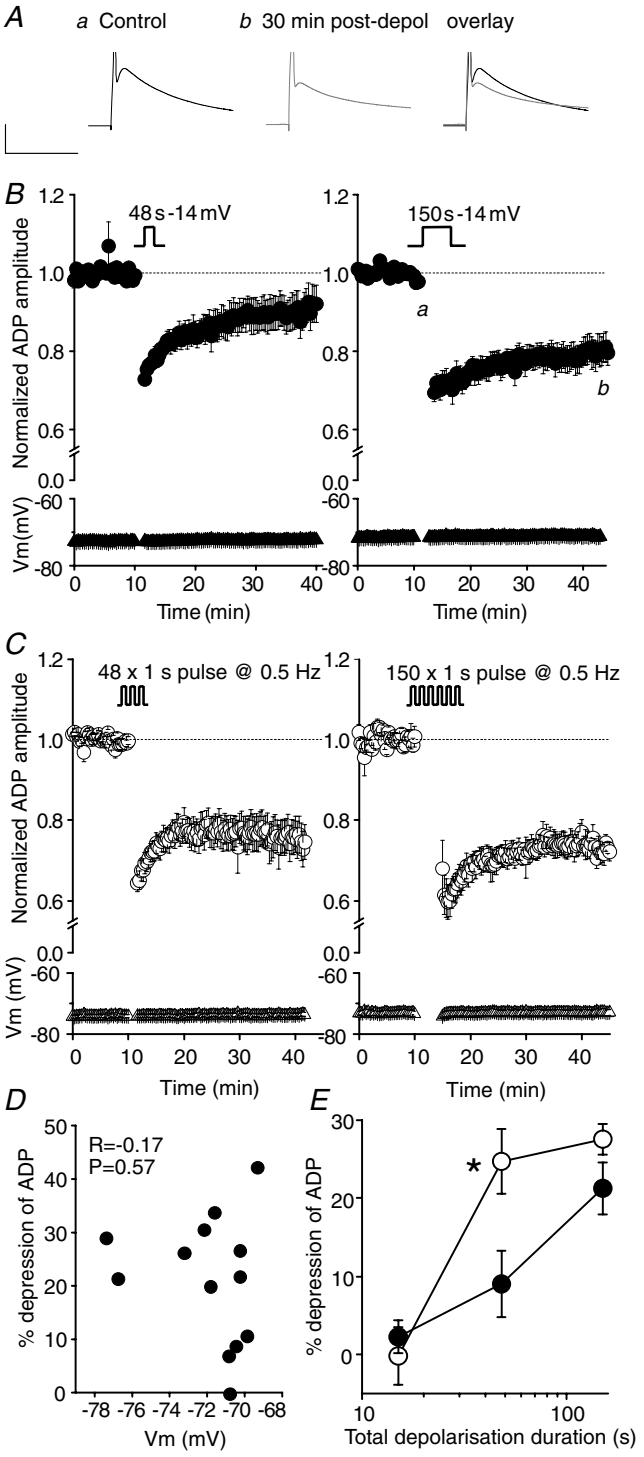

Figure 3. Transient depolarization results in a long-term depression of the ADP
A, traces from a single experiment showing the prolonged (30 min) depression in ADP amplitude following a transient (150 s) depolarization from a holding potential of −84 mV to −14 mV. Calibration: 50 ms, 10 mV. *B*, pooled data describing the effect of a transient depolarization on ADP amplitude. After obtaining a stable baseline for 10 min, the amplifier was switched to voltage clamp mode and the cell continuously depolarized from −84 mV to −14 mV for 48 s (left; $n = 13$) or 150 s (right; $n = 13$). Following the conditioning stimulus, the amplifier was switched back to current clamp mode and the resulting change in ADP monitored for a further 30 min. During current clamp recordings the membrane potential of each cell was maintained close to its initial resting level by automatic somatic current injection, such that the ADP did not initiate a secondary spike. The mean membrane potentials for each data set are plotted at the bottom of each graph (triangular symbols). *C*, pooled data generated using a similar protocol as described in *B*. However, in these experiments the cells were depolarized in a phasic, 'bursting' pattern, consisting of repetitive depolarizing voltage steps (1 s duration) from −84 mV to −14 mV, repeated either 48 (left; $n = 10$) or 150 (right; $n = 5$) times, at 0.5 Hz. *D*, scatter plot showing the lack of relationship between the resting membrane potential of the neuron and the extent of depolarization-induced plasticity. *E*, pooled data demonstrating that the extent of depolarization-induced long-term plasticity (measured 30 min after the depolarizing stimulus) is dependent on the duration of depolarization for both phasic (open symbols) and tonic (filled symbols) stimuli. Phasic stimulation for 48 s resulted in a significantly larger depression of the ADP when compared to a continuous depolarization of the same duration (*$P < 0.05$, unpaired *t* test).

Fig. 3*B*). A depolarizing conditioning stimulus lasting only 15 s produced only a transient depression ($17.6 \pm 1.8\%$ depression; $P < 0.05$, $n = 5$) of the ADP that decayed away over ∼10 min ($2.3 \pm 2.1\%$ depression; $P = 0.4$, $n = 5$). Voltage clamping the membrane potential at −84 mV for 150 s (i.e. without depolarizing the cell) did not result in either a transient or long lasting suppression of the ADP ($97 \pm 2\%$ of baseline after 30 min; $n = 3$; Fig. 4). Depression of the ADP by tonic depolarizing conditioning stimuli was not associated with any significant post-conditioning change in resting membrane resistance, time constant or the current required to maintain the cell at the set resting potential. Furthermore, there was no correlation between the set resting potential and the degree of depression induced by conditioning (Fig. 3*D*).

In addition to eliciting persistent changes to the ADP with conditioning stimuli consisting of tonic depolarizations, we also examined equivalent phasic conditioning protocols. Here 1 s depolarizations to −14 mV were alternated with an identical period at −84 mV. Phasic conditioning protocols produced no change in basic membrane properties of cells, similar to their tonic counterparts. However, as illustrated in Fig. 3*C*, phasic depolarizations were also capable of inducing a prolonged depression of the ADP. For instance, prior to a conditioning stimulus which consisted of 150, 1 s depolarizations, the mean ADP amplitude was 16.0 ± 1.8 mV, whilst 30 min after conditioning, the ADP amplitude was 11.5 ± 1.1 mV, a reduction of $27.5 \pm 2.0\%$ ($P < 0.01$, $n = 5$). Interestingly, the protocol employing intermittent depolarizations appeared to be more efficacious, since it produces near maximal ADP depression for 48 s of total depolarization ($24.7 \pm 4.2\%$ depression 30 min after depolarization; $P < 0.05$, $n = 10$; Fig. 3*E*).

In the experiments described above we were careful to ensure the control ADP did not reach spike threshold and elicit secondary action potential firing, like that shown in Fig. 1*E* and *F*. As detailed in the Methods this was achieved by appropriately setting the resting membrane potential with automatic slow current injection. To illustrate the functional consequences of ADP depression on cell firing behaviour, however, an example experiment in which the ADP prior to conditioning was permitted to evoke an additional action potential is shown in Fig. 5. Here following application of a conditioning stimulus composed of a 150 s depolarization to −14 mV, the subsequently depressed ADP consistently failed to elicit a second action potential, consequently halving the number of action potentials produced in response to the invariant test stimulus of 2 ms injection of 2 nA.

Long term intrinsic plasticity induced modulation by theta burst action potential firing

The voltage clamp-based conditioning stimuli used above to induce changes to burst firing and depression of the ADP in CA3 cells are probably more representative of pathological voltage transients than those seen during normal behaviour (see Discussion). Consequently, we were minded to investigate if similar intrinsic plasticity and depression of the ADP could be evoked if physiologically feasible patterns of neuronal activity were used as a conditioning stimulus. To do this we applied conditioning stimuli in current clamp mode. These consisted of brief suprathreshold current injections designed to produce action potential firing reminiscent of active hippocampal place cells. Specifically, we used series of 2 ms current injections to produce bursts of spikes consisting of either two or four action potentials. These bursts were applied at a burst frequency of either 5 or 10 Hz (i.e. theta frequency) for a conditioning period of 1 min. The intraburst spike intervals were matched to those of the average initial spike burst produced by injecting 200 pA current into CA3 cells (i.e. either the first 1 or 3 spike intervals shown in Fig. 1*B*). During the application of these theta burst firing (TBF) conditioning stimuli, the automatic slow current injection facility used during ADP measurements was disabled, thus permitting the cell's membrane potential to follow its desired course.

In all such experiments TBF conditioning stimuli were able to induce a long-lasting depression the ADP triggered in response to spikes triggered by single 2 nA, 2 ms current injections. For example, prior to TBF (bursts of 4 action potentials delivered at 10 Hz), the mean ADP amplitude was 16.1 ± 1.0 mV, whereas 30 min after TBF, the mean ADP amplitude was 12.2 ± 0.8 mV ($P < 0.01$, $n = 12$; Fig. 6*A*). Furthermore, each of the TBF protocols tested

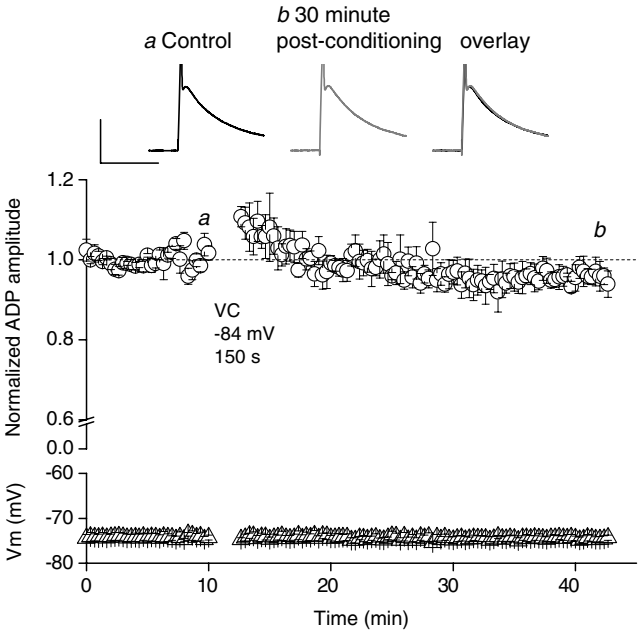

Figure 4. Voltage clamping at hyperpolarized membrane potentials does not result in depression of the ADP
The traces show the ADP before and 30 min after voltage clamping at a hyperpolarized membrane potential (−84 for 150 s). Calibration: 10 mV, 50 ms. Pooled data showing the lack of effect of a hyperpolarizing voltage clamp protocol on the ADP amplitude ($P = 0.3$, $n = 3$).

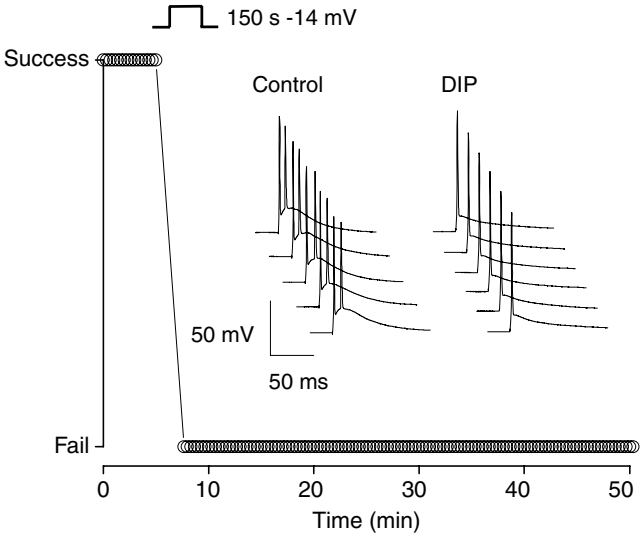

Figure 5. Depolarization-induced plasticity can alter the burst-firing properties of CA3 pyramidal neurons
The traces shown are consecutive example sweeps from a CA3 pyramidal neuron in which the ADP was sufficiently large to drive a second action potential. This cell was maintained at −71 mV. Following transient depolarization in voltage clamp mode from −84 to −14 mV, the ADP amplitude was reduced and the secondary action potential firing completely suppressed. The graph plots the success or failure rate of secondary action potential firing, before and after the conditioning depolarization.

also modified the burst architecture observed in response to 500 ms, 200 pA current injections. For instance, 30 min after a TBF protocol consisting of bursts of four action potentials delivered at 10 Hz, the first ISI increased by 12.2 ± 2.9 ms ($P < 0.05$, $n = 7$; Fig. 6*B*). Indeed, the changes produced in both ADP amplitude and first ISI were very similar in magnitude to those generated by the most effective of our voltage clamp-based conditioning protocols (Fig. 3). Summary data describing the effects on ADP amplitude and first ISI of three different 1 min TBF conditioning stimuli are presented in Fig. 6*C* and *D*, respectively. No significant difference was detected between the different TBF stimulation paradigms.

As well as increasing the first ISI these TBF conditioning stimuli also produced associated long-lasting increases in mean spike jitter. Thus, prior to TBF, the mean jitter of the first ISI was 1.20 ± 0.31 ms, whereas 30 min after TBF the mean jitter was significantly increased to 2.01 ± 0.34 ms ($P < 0.05$; data not shown). Similar to plasticity elicited with voltage-clamp, theta burst-induced persistent intrinsic plasticity was not associated with changes to input resistance or the amount of current required to maintain the cell at its set resting potential. It thus appears that firing patterns which mimic the physiological firing of CA3 cells are also able to induce long-lasting intrinsic plasticity, suggesting that this phenomenon may be a pertinent feature of normal hippocampal information processing and plasticity.

Intrinsic plasticity of spikes driven by suprathreshold EPSP-like depolarizations

Above we have described alterations to the firing patterns and/or ADPs of CA3 neurons stimulated with either short, strong depolarizations (2 nA, 2 ms) that elicit a spike and subsequent ADP, or much longer depolarizing current injections (200 or 300 pA for 500 ms) that generate an initial burst of spikes followed by lower frequency firing. Physiologically, neurons are not excited to threshold by such 'square-wave' current injections but are instead usually depolarized by excitatory synaptic inputs. To demonstrate that CA3 cells will respond to synaptic

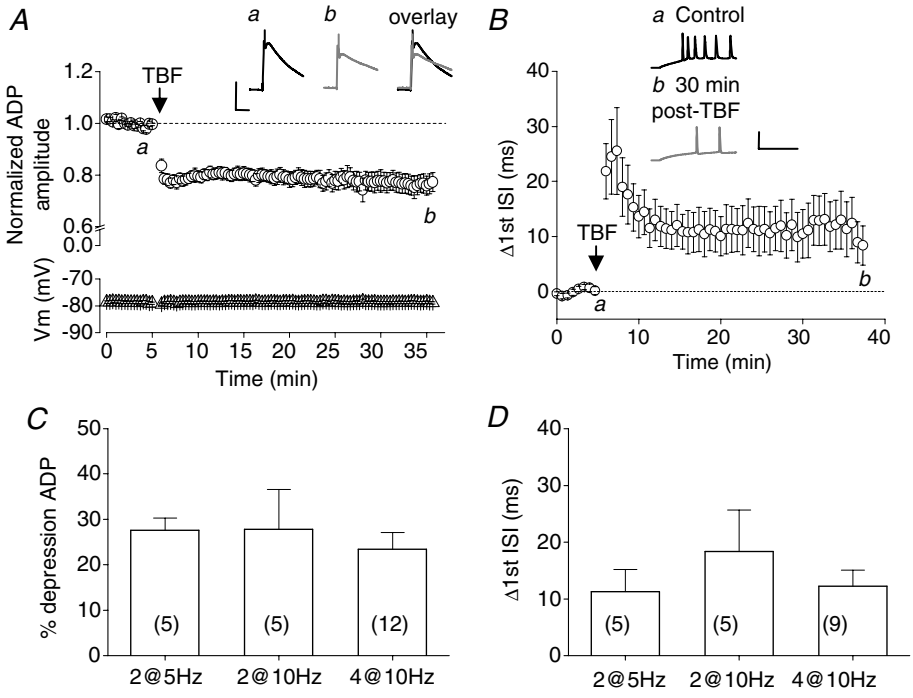

Figure 6. Theta frequency burst firing results in persistent intrinsic plasticity
A, pooled data ($n = 12$) showing the long term depression of the ADP in response to a brief (60 s) period of theta frequency burst firing (TBF; a burst of 4 APs delivered at 10 Hz; see Methods). Example traces show an ADP and truncated action potential before (black trace) and 30 min after TBF (grey trace). Calibration: 10 mV, 50 ms. *B*, traces show the initial portion of a response to a 200 pA, 500 ms current injection, before (black trace) and after (grey trace) TBF. Note the slowing of action potential firing. Calibration: 50 mV, 50 ms. Pooled data ($n = 9$) showing the increase in the first interspike interval following TBF. *C*, a variety of TBF protocols induce significant levels of intrinsic plasticity (2@5 Hz: 2 APs delivered at the mean intrinsic burst frequency repeated at 5 Hz for 60 s; etc.). The bars represent the change in ADP amplitude. *D*, the TBF protocols that produced depression of the ADP also produced a persistent change in first ISI 30 min after conditioning. In *C* and *D* no significant difference between the 3 TBF protocols was observed ($P > 0.05$; *n* numbers shown on figure).

inputs with a burst, we used the sum of exponentials to construct current injection templates that approximate the time course of typical glutamate receptor-mediated EPSCs of CA3 pyramidal cells. These were then used as depolarizing stimuli in current clamp recordings. Such stimuli produce a response that resembles a somatically recorded EPSP (Fig. 7*A*). When the current stimulus was made large enough to trigger action potential firing, multiple action potentials in a high frequency burst were invariably produced (Fig. 7*A*).

Traces from an example recording in which the outcomes of EPSC-like stimuli of various decay rates were investigated are shown in Fig. 7*B*. It is apparent that the behaviour of the burst thus generated reflected the time course of the EPSC-like waveform used as a stimulus, but importantly a burst was always observed.

We next investigated the effects of a TBF conditioning protocol on spiking activity driven by suprathreshold EPSC-like waveforms. During a 5 min baseline period, suprathreshold EPSC-waveforms induced an average of 2.6 ± 0.2 action potentials ($n = 9$). Immediately after a TBF protocol (bursts of 2 spikes at 10 Hz for 60 s), the number of spikes induced by an identical EPSC-like waveform was reduced by ~50%. The reduction in spike number was maintained, such that 30 min after conditioning, there were still significantly fewer spikes in response to an EPSC-like waveform (1.9 ± 0.2 spikes; $n = 9$, $P < 0.01$; Fig. 7*C*). In two of these nine neurons, the TBF protocol reduced firing to such an extent that post-conditioning the EPSC-like current injection was only capable of inducing a solitary spike. In the other seven cells, the interval

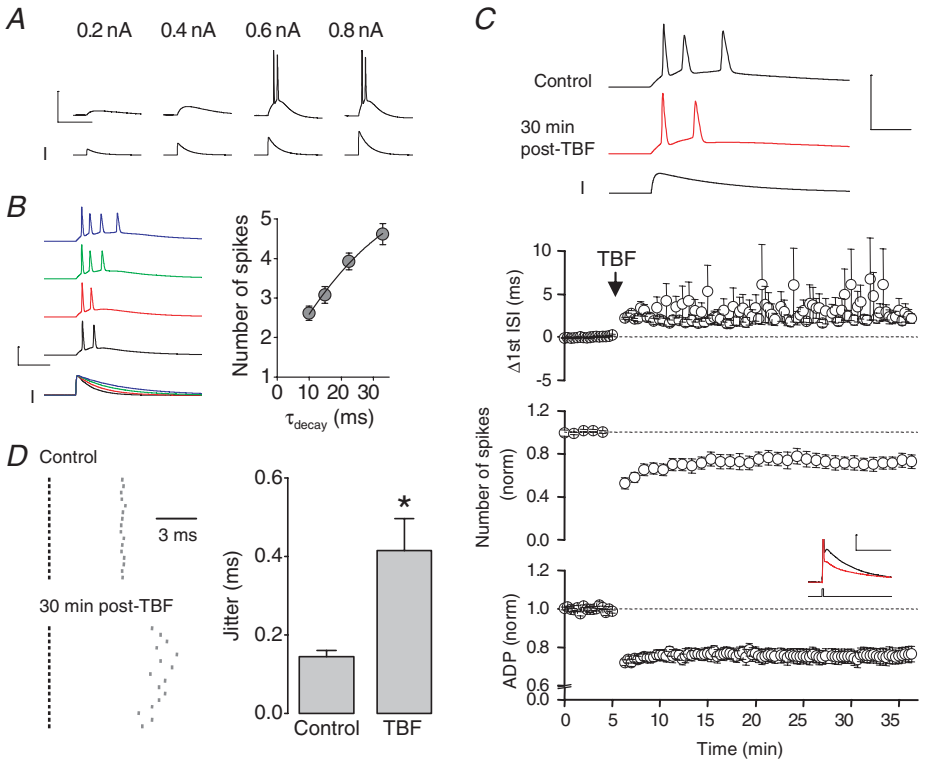

Figure 7. Persistent intrinsic plasticity changes firing induced by suprathreshold EPSC-like current injections

A, current injections consisting of the sum of two exponentials were used to model a depolarizing synaptic waveform. The peak amplitude of the 'EPSC-like' waveform was monotonically increased until action potentials were observed. In general, the EPSC-like waveform (with a decay constant of 15 ms) always resulted in a burst of 2–5 action potentials. *B*, an increase to the decay constant, increased the number of spikes observed in response to the EPSC-like waveform ($n = 13$). *C*, traces exemplify the increase in the interval between the first 2 spikes evoked by an EPSC-like waveform, following a theta-burst firing protocol (a burst of 2 spikes at high frequency delivered at 10 Hz for 60 s). Furthermore, there is a reduction in the number of spikes. Calibration 10 ms, 100 mV. Pooled data illustrate the significant change ($P < 0.01$) in normalized number of spikes ($n = 9$) and ADP amplitude ($n = 9$). In 2 cells, the TBF protocol eliminated secondary spike firing induced by the EPSC-like waveform. In the remaining 7 cells, the interval between the first two spikes was significantly increased ($P < 0.05$, $n = 7$). *D*, furthermore, the spike-timing reliability, measured as the jitter of the first ISI was significantly reduced following TBF ($P < 0.05$, $n = 7$). The first spikes are represented by the black lines, the second spikes by the grey lines. The timing of the second spike is shown relative to the first spike.

between the first two spikes was significantly increased from 5.4 ± 0.1 ms pre-conditioning to 7.3 ± 0.5 ms 30 min post-conditioning ($n = 7$, $P < 0.05$; Fig. 7*C*). Furthermore, the spike timing reproducibility was significantly reduced, such that during the baseline the jitter of the first ISI was 0.14 ± 0.02 ms, which increased to 0.41 ± 0.08 ms ($n = 7$, $P < 0.05$) 30 min after application of the TBF protocol (Fig. 7*D*). These changes are paralleled by a reduction in the ADP in the same cells ($24.3 \pm 4.0\%$ reduction in ADP amplitude; $n = 9$, $P < 0.05$; Fig. 7*C*).

Mechanisms involved in generation of intrinsic plasticity

Having identified a novel form of intrinsic plasticity in CA3 neurons we have started to investigate the mechanisms through which this process occurs. For these studies we concentrated our experiments on conditioning-induced changes to the ADP. Many forms of synaptic and intrinsic plasticity are known to rely on an increase in postsynaptic intracellular Ca^{2+} (Bliss & Collingridge, 1993; Aizenman & Linden, 2000; Tsubokawa *et al.* 2000; Lei *et al.* 2003; Fan *et al.* 2005). Indeed, all of the various conditioning stimuli we used to induce the persistent changes in CA3 excitability are likely to generate substantial increases in intracellular Ca^{2+} via activation of somatic voltage-gated Ca^{2+} channels. We consequently tested if inclusion of a high concentration of the fast Ca^{2+} buffer BAPTA (10 mM) in the pipette solution could modify conditioning induced depression of the ADP. A robust ADP was observed when recording with 10 mM intracellular BAPTA (ADP amplitude, 19.9 ± 1.6 mV; $n = 5$) but its depression by TBF was completely eliminated (ADP amplitude 30 min post-TBF, 19.2 ± 1.1 mV; $n = 5$, $P = 0.4$; Fig. 8*A*). This suggests a key role for increases in cytoplasmic Ca^{2+} in the induction of this form of persistent plasticity.

In CA1 cells a long-lasting form of intrinsic plasticity can also be triggered by theta frequency burst firing, an effect involving an NMDA receptor-dependent up-regulation of the non-selective cation conductance I_h and change in input resistance (Fan *et al.* 2005). Mechanistically this change in CA1 cells is clearly distinct from the plasticity in CA3 neurons we describe here, since our form of plasticity is not NMDA receptor dependent and does not result in a measurable change in input resistance. Despite this we were still interested in testing for an involvement of I_h. In CA3 cells a high concentration of the I_h blocker ZD2788 (20 μM) had no effect on the ADP alone or on its modification by a conditioning stimulus (Fig. 8*B*). ZD2788 did, however, successfully eliminate the characteristic sag produced by I_h activation during hyperpolarizing current injections (data not shown).

The ensemble of ionic conductances that generate the ADP in CA3 pyramidal cells has not, as yet, been well characterized. ADPs in other pyramidal cells are reported to include contributions from various currents including

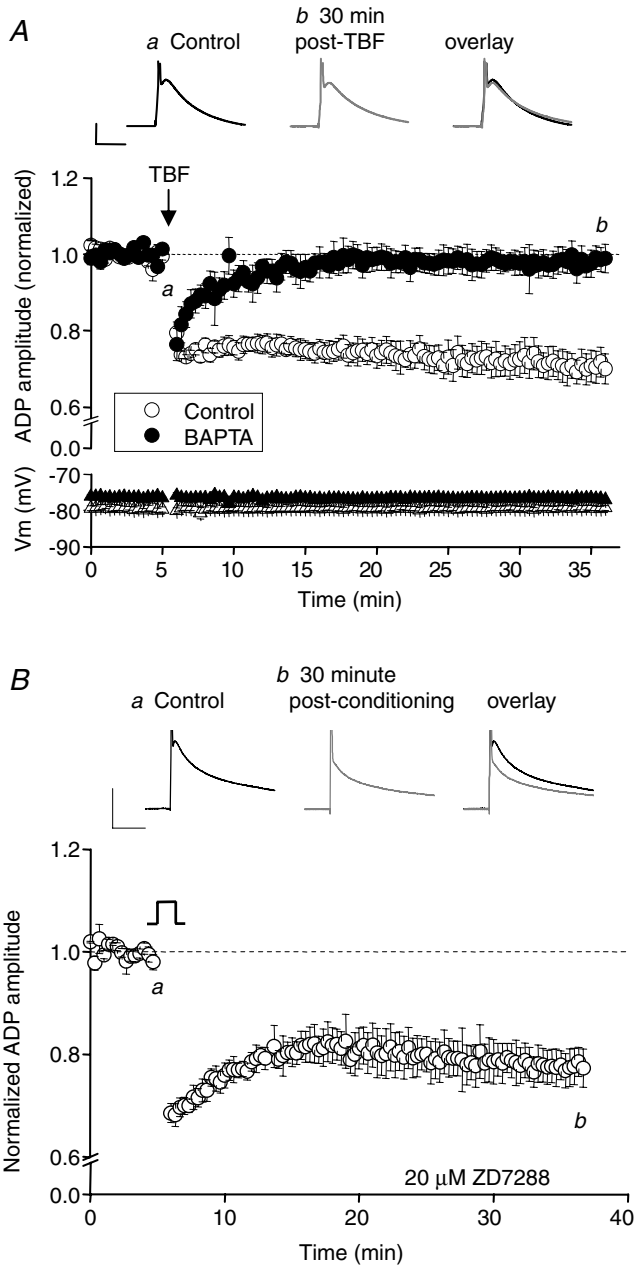

Figure 8. Intracellular BAPTA, but not extracellular ZD7288, blocks the TBF-induced change in ADP
A, pooled data shows the lack of long term depression of the ADP in the presence of intercellular BAPTA (10 mM; $n = 5$) compared with interleaved control experiments ($n = 5$). Traces are from an example experiment in the presence of intracellular BAPTA (10 mM). Calibration 10 mV, 20 ms. *B*, the traces show the ADP before and after transient depolarization (−84 to −14 mV for 2.5 min) in the presence of the I_h blocker ZD7288 (20 μM). Calibration: 10 mV, 50 ms. Pooled data show that significant intrinsic plasticity can still occur in the continuous presence of ZD7288 ($P < 0.05$; $n = 3$).

persistent Na^+ currents (Yue *et al.* 2005), R-type Ca^{2+} currents (Metz *et al.* 2005), D-type K^+ currents (Metz *et al.* 2007) and Ca^{2+}-activated non-selective (CAN) cation channel currents (Caeser *et al.* 1993). One potentially interesting contribution to the ADP arises from Kv7 channels, which appear to be responsible for terminating the ADP in CA1 cells (Yue & Yaari, 2004; Chen & Yaari, 2008) and CA3 cells (Vervaeke *et al.* 2006). In line with these studies, we find that the ADP in CA3 pyramidal cells is enhanced ($15.9 \pm 3.5\%$ increase; $n = 4$, $P < 0.05$) by the selective Kv7 channel blocker XE991 (10 μM; Fig. 9*A*). Furthermore, retigabine a compound that enhances Kv7 channel gating (Main *et al.* 2000; Rundfeldt & Netzer, 2000; Wickenden *et al.* 2000; Tatulian *et al.* 2001), depresses the ADP ($18.7 \pm 3.2\%$ decrease; $n = 10$, $P < 0.01$) and in parallel unmasks a mAHP (Gu *et al.* 2005; Fig. 9*B*).

The consequences for the ADP of inducing our novel form of intrinsic plasticity and applying retigabine

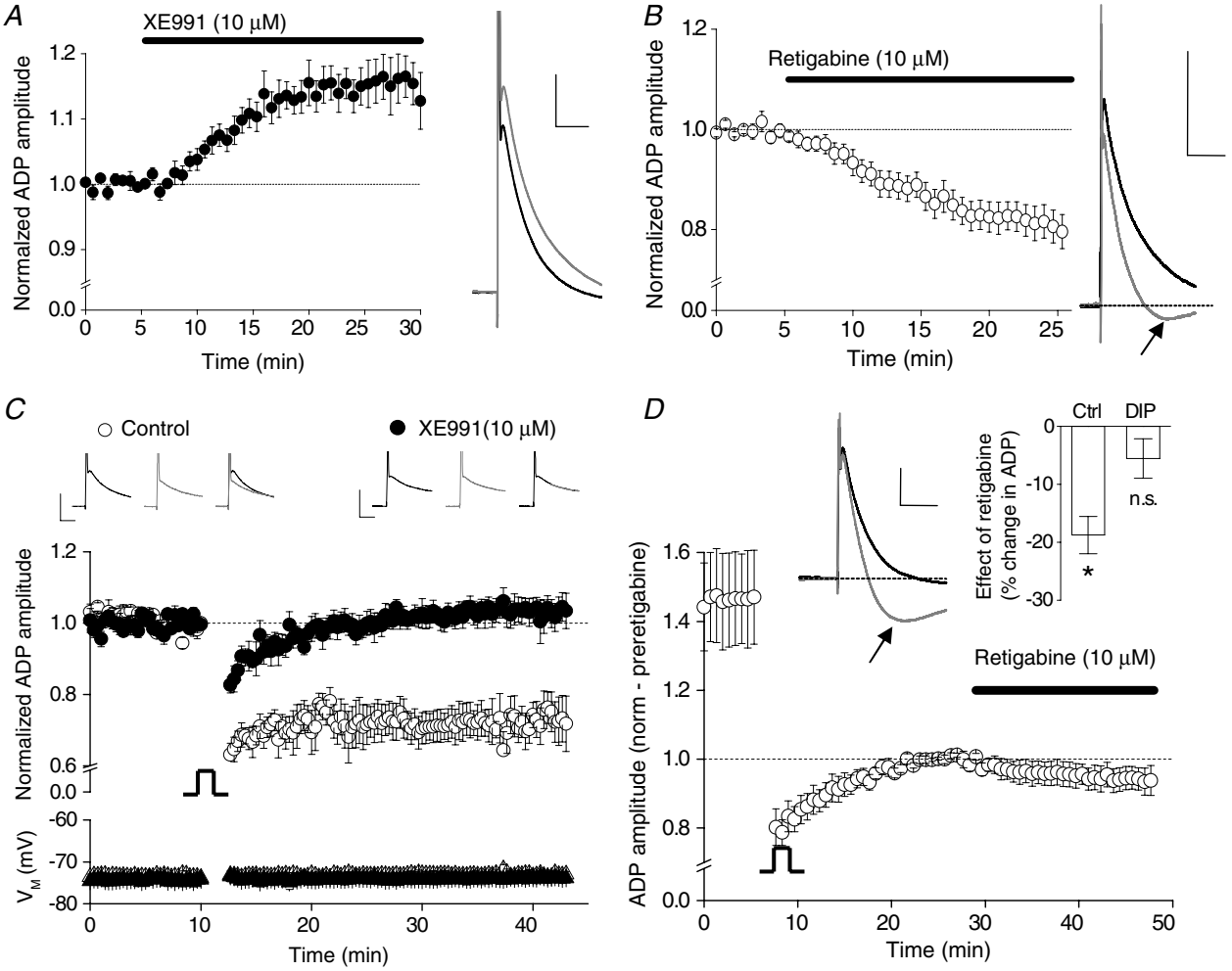

Figure 9. Inhibition of Kv7/KCNQ channels abolishes persistent intrinsic plasticity
A, a recording of an ADP from a CA3 pyramidal neuron under control conditions (black trace). Following bath application of the Kv7 channel blocker XE991 (10 μM), the ADP is enhanced (grey trace). Calibration: 50 ms, 5 mV. The pooled time course of this change in ADP ($n = 4$, $P < 0.05$) is shown on the left. *B*, pooled data showing the reduction in ADP amplitude by the Kv7 channel opener retigabine (10 μM; $n = 10$). The example trace shows the ADP before and 20 min after (black and grey trace respectively) application of retigabine. Note the appearance of a mAHP following the addition of retigabine (arrow). Calibration: 10 mV, 100 ms. *C*, transient depolarization (150 s; −84 to −14 mV) in the presence of XE991 (10 μM; preapplied for at least 20 min) does not result in depression of the ADP ($n = 6$, $P > 0.05$), whereas substantial depression was observed in 4 interleaved control experiments (i.e. in the absence of XE991). Calibration: 20 ms, 10 mV. *D*, once a stable baseline was achieved following induction of intrinsic plasticity (20 min post-conditioning stimulus), retigabine failed to significantly modulate the ADP amplitude. However, retigabine still induced an mAHP (see example traces). Calibration: 5 mV, 50 ms. Inset: 20 min application of retigabine results in a significant ($P < 0.05$, $n = 10$) depression of the ADP in control conditions but no significant change following the induction of intrinsic plasticity ($P > 0.05$, $n = 6$).

treatment appear very similar. This suggested to us that a key feature of the conditioning-induced change could be persistent modulation of Kv7 channel activity. Consequently we examined how treatment with Kv7 channel modulators changed conditioning-induced depression of the ADP.

Following preincubation in XE991 for at least 20 min prior to starting a recording, the ADP amplitude was 14.6 ± 0.7 mV ($n = 6$). The ADP amplitude was stable throughout the 10 min baseline period prior to application of the conditioning stimulus (Fig. 9*C*), which consisted of a 250 s depolarization to −14 mV. Following conditioning, the ADP was transiently depressed, but rapidly returned to pre-conditioning amplitude within ∼5 min. Consequently, 30 min post-conditioning, the ADP amplitude was not significantly different from its pre-conditioning level (15.1 ± 1.0 mV; $n = 6$, $P = 0.4$). In interleaved control experiments, performed in the absence of XE991, the ADP was significantly depressed by the same depolarizing conditioning stimulus (baseline ADP amplitude, 13.5 ± 0.8 mV; 30 min post-depolarization, 10.0 ± 1.2 mV; $n = 4$, $P < 0.01$; Fig. 9*C*). This indicates that the conditioning-induced depression of the ADP we have identified is mediated by a long-term modification to Kv7 channel gating. Further supporting a role for Kv7 channels in intrinsic plasticity, we found that 20 min after inducing the plastic change, retigabine was no longer able to significantly reduce the amplitude of the ADP ($5.5 \pm 3.4\%$ depression, $n = 6$, $P = 0.2$; *vs.* $18.7 \pm 3.2\%$ depression in control; $n = 10$, $P < 0.05$; Fig. 9*D*). In contrast, retigabine was still capable of enhancing the mAHP (Fig. 9*D*) suggesting that Kv7 channel activity had not simply been 'washed out' as a consequence of whole-cell recording.

Discussion

We have identified a novel form of depolarization-induced, long-lasting intrinsic plasticity in hippocampal CA3 pyramidal neurons. This plastic change is manifest as both a change to the burst firing properties of CA3 cells and a depression of the ADP. In our initial experiments, plasticity was induced by conditioning stimuli consisting of defined periods during which the cell was voltage clamped at −14 mV. Here the extent of the plastic change was related to the duration of the depolarizing conditioning stimulus, indicating that this process of intrinsic plasticity is graded in nature (Fig. 3*E*). Furthermore, phasic conditioning protocols, in which periods at −14 mV were alternated with periods at −84 mV, appeared more efficacious than tonic depolarizations. We hypothesize that the phasic protocol may be more effective than its tonic counterpart because it could induces cycles of voltage-dependent inactivation and de-inactivation of a membrane conductance crucially involved in the induction process, where tonic depolarization would simply generate inactivation.

Potential routes to intrinsic plasticity *in vivo*

Conditioning stimuli consisting of tonic or phasic depolarizations applied in voltage clamp are unlikely to represent typical physiological activity in CA3 cells. They do, however, approximate the type of changes in membrane potential seen in pathological conditions. Brain ischaemia, for example, is well known to elicit profound depolarization of neuronal tissue (Somjen, 2001). Indeed, it is likely that patients suffering stoke will experience more prolonged periods of neuronal depolarization than those required to produce intrinsic plasticity in CA3 cells. Similarly, spreading depression, a process thought to reflect the pathophysiology of migraine, produces repetitive periods of profound neuronal depolarization in cortical areas (Somjen, 2001). These episodes individually last from tens to hundreds of seconds (Sugaya *et al.* 1975; Snow *et al.* 1983). Hippocampal area CA3 is particularly prone to generating epileptiform discharges (Green, 1964; Ben-Ari, 1985). The depolarization associated with epileptic seizures is also a good candidate to engage the intrinsic plasticity we have described here, especially since the phasic depolarization pattern (which induced plasticity in a more efficient fashion) crudely mimics the type of complex depolarizing waveform associated with ictal episodes. It is also worthy of note that the killing of rodents and subsequent preparation of brain slices are processes that will doubtless cause prolonged bouts of depolarization of neuronal tissue. Consequently, the ADP and excitability of CA3 pyramidal cells in brain slice preparations may already be partially depressed as a result of inducing intrinsic plasticity during tissue preparation.

In addition to inducing persistent intrinsic plasticity by depolarizing CA3 cells with voltage clamp techniques, a seemingly identical process could be induced by making CA3 cells fire bursts of action potentials at theta frequency. The patterns of cell firing we used to induce plasticity in this way were designed to mimic the firing activity of hippocampal place cells. Thus, it seems our the plastic change we have identified can be induced by patterns of activity that may arise physiologically as well as pathologically.

Functionally, the intrinsic plasticity we have identified is expressed in a number of ways. Changes were observed in responses to short (2 ms), strong (2 nA) suprathreshold current injections, to current injections designed to mimic EPSC waveforms, and to more prolonged (500 ms) supratheshold stimuli. A key feature of the plastic process is a robust, long-lasting depression of the ADP. The ADP is a key component in the generation of action potential bursts

by hippocampal pyramidal cells (Yue & Yaari, 2004; Yue *et al.* 2005; Metz *et al.* 2007). Consequently, a long-lasting, activity-dependent modulation of the ADP is likely to have significant consequences for the functional neurophysiology of CA3 cells and their various downstream synaptic targets.

The intrinsic plasticity described here was associated with a significant increase in the interval between the first two action potentials generated by more prolonged test stimuli including the mock-synaptic current injections shown in Fig. 7. Although an ADP is not readily observable unless current injections are rapidly terminated and the membrane allowed to discharge, the conductances that underpin the ADP remain key in controlling the first few spikes produced by longer depolarizing stimuli (Fig. 1). Thus, we believe the profound changes to spike firing frequency in the initial action potential burst triggered by prolonged current injections reflect the same processes that depress the ADP.

Mechanisms underlying intrinsic plasticity

To date, there have been relatively few reports of long term neuronal plasticity induced by transient somatic depolarization alone. Long term depression of both ionotropic (Lei *et al.* 2003) and metabotropic (Jin *et al.* 2007) glutamate receptor-mediated synaptic transmission can be induced by depolarization. Intrinsic plasticity induced by membrane depolarization has been reported in layer V neurons of the entorhinal cortex, but only in the presence of a muscarinic acetylcholine receptor agonist (Egorov *et al.* 2002). In CA1 pyramidal cells, action potential bursts applied at theta frequency decrease excitability via modulation of I_h, a process that is NMDA receptor dependent (Fan *et al.* 2005). Notably, all our experiments were carried out with blockers of NMDA, AMPA/kainate and $GABA_A$ receptors present. Thus, circuit effects and consequent synaptic signalling in the strongly interconnected CA3 network seem an unlikely source for the depolarization-induced change in the ADP. Also our form of intrinsic plasticity is insensitive to the I_h blocker ZD7288 and is thus distinct from the activity-dependent plastic changes described in CA1 cells reported by Fan *et al.* (2005). Recently another form of Kv7 channel-sensitive intrinsic plasticity has been reported in CA1 pyramidal neurones, although this appears to be markedly different in nature from the plasticity observed here (Wu *et al.* 2008). For example, the authors show that a conditioning stimulus results in an alteration to spike number, but no change to burst firing, unlike the data presented here.

Our observations strongly suggest that modulation of Kv7 channels underlies conditioning-induced depolarization of the ADP. We have not yet established, however, a suitable voltage-clamp protocol to demonstrate directly conditioning-mediated modification of Kv7 channel gating. The major hindrance to this endeavour is the nature of standard voltage clamp protocols used to measure Kv7 channels. These involve clamping the cell at depolarized membrane potentials and identifying the Kv7-mediated conductance through its deactivation trajectory observed in response to a hyperpolarizing step. Unfortunately for our purposes, clamping the cell at a depolarized potential to measure M-current will in itself cause the persistent plastic changes we described here (e.g. Figs 2 and 3). Indeed, for this reason previous voltage clamp studies of M-currents in some cells may actually be of channels that have been pre-conditioned by the very protocol used to study them. A potential alternative voltage-clamp based approach is to study depolarization-induced activation of Kv7 currents. We have, however, not been able to identify conditions under which we can confidently isolate a Kv7-mediated current from the plethora of other voltage-gated K^+ currents of CA3 pyramids.

A common feature shared by depolarization-driven synaptic or intrinsic plasticity is a reliance on an increase in intracellular Ca^{2+} concentration (Lei *et al.* 2003; Fan *et al.* 2005; Jin *et al.* 2007). By increasing gating of voltage-sensitive Ca^{2+} channels, all the effective conditioning protocols described here will unquestionably increase intracellular Ca^{2+}. By buffering intercellular Ca^{2+} with BAPTA we were readily able to establish a central role for Ca^{2+} in the induction of this form of intrinsic plasticity.

Downstream from an activity-dependent increase in Ca^{2+}, our data strongly point towards a long-term modulation of Kv7 channels as central to the production of intrinsic plasticity. Specific Kv7 channel blockers such as XE991 are potential cognitive enhancers (Zaczek *et al.* 1998) and enhance the ADP (Yue & Yaari, 2004; Vervaeke *et al.* 2006), whereas retigabine, a drug that facilitates Kv7 channel opening (Main *et al.* 2000; Rundfeldt & Netzer, 2000; Wickenden *et al.* 2000; Tatulian *et al.* 2001) and impairs memory (Korsgaard *et al.* 2005), depresses the ADP (Yue & Yaari, 2004; Vervaeke *et al.* 2006). When XE991 was used to block Kv7 channels, a conditioning protocol effective under control conditions failed to depress the ADP. In other experiments we found that following the induction of intrinsic plasticity retigabine was no longer able to significantly depress the ADP. We therefore suggest that a major mechanism underpinning conditioning-mediated depression of the ADP, and consequent effects on firing patterns, is an increased ability of Kv7 channels to curtail the ADP. In this way, the process of intrinsic plasticity described here produces an outcome for the ADP that parallels the pharmacological actions of anticonvulsant Kv7 channel openers (Yue & Yaari, 2004; Vervaeke *et al.* 2006), and thus potentially represents an endogenous anti-convulsant mechanism

within the CNS. Interestingly, a recent paper (Chen & Yaari, 2008) describes how Ca^{2+} entry from single action potentials transiently inhibits Kv7 channels leading to an enhanced ADP and burst generation. Thus, Ca^{2+} ions may have a dual role in regulation of the ADP: a short-term enhancement via Kv7 channel inhibition and a long term inhibition via a retigabine-like effect. In summary, we propose that Kv7 channel function is in some way upregulated by the depolarizing conditioning stimuli; as a result, further enhancement of Kv7 activity by retigabine is largely occluded.

The ion channels that generate the ADP in CA3 pyramidal neurones are not well characterized. In CA1 pyramidal neurones, which are morphologically, physiologically and pharmacologically distinct from CA3 cells, the ADP appears to be driven by a persistent Na^+ current (Yue *et al.* 2005) and/or an R-type Ca^{2+} current (Metz *et al.* 2005). It is possible, therefore, that the intrinsic plasticity described in this study represents some form of plasticity of the channels underlying these currents. It is worth pointing out, however, that the ADP in CA3 neurones is insensitive to riluzole (J. T. Brown and A. D. Randall, unpublished observations), a blocker of the persistent Na^+ current (Urbani & Belluzzi, 2000). This suggests that the persistent Na^+ current does not play a major role in the ADP of CA3 neurones.

Importance of persistent intrinsic plasticity in hippocampal networks

Finally, we must consider the potential relevance of the persistent intrinsic plasticity we have identified to hippocampal function. As stated above, activity-dependent depression of the ADP has the potential to provide a feedback protective function, reducing pro-convulsive burst firing in the highly interconnected CA3 network. We show that spiking activity induced by suprathreshold EPSC-like waveforms is modulated in a lasting fashion following the induction of intrinsic plasticity. This would presumably lead to changes in downstream synaptic output at the tens of thousands of synapses each CA3 cell makes with other neurons throughout areas CA1, CA2 and CA3 of the ipsi- and contra-lateral hippocampi, as well as at extra-hippocampal sites, most notably the lateral septal nucleus (Amaral & Lavenex, 2007; Wittner *et al.* 2007).

Such alterations to firing behaviour are likely to affect short term synaptic plasticity at CA3 cell synaptic terminals and the summation of EPSPs in target cells. Induction of long term potentiation (LTP) at CA3–CA1 synapses is dependent on high frequency activity in the presynaptic CA3 neurons (Dudek & Bear, 1992). Our findings indicate that CA3 neurons which have undergone a conditioning-dependent intrinsic plasticity (for example during a seizure) may no longer be able to fire action potentials at such high frequencies, and thus may have an impaired potential to produce LTP. In this context, it is noteworthy that both LTP and learning are impaired in rats which have undergone experimentally induced seizures (Zhou *et al.* 2007). Indeed, patients with idiopathic generalized epilepsy exhibit memory impairments, which occur independently from macroscopic neuronal death (Dickson *et al.* 2006). With respect to changes to spike reliability, a recent report suggests that CA3 neurons from rodents which have undergone experimentally induced seizures show a reduction in spike-timing reliability, which modulated subsequent neuronal network activity (Foffani *et al.* 2007).

In summary, we have identified a novel, Ca^{2+}- and Kv7 channel-dependent, long-lasting form of intrinsic plasticity in CA3 pyramidal cells. The changes this process elicits may have substantial neurophysiological consequences for both CA3 cells and their downstream synaptic targets. Much more work is required to uncover the precise biochemical pathways involved in this form of intrinsic plasticity and to investigate its relevance to the physiological and pathological behaviour of the hippocampus *in vivo*.

References

Aizenman CD & Linden DJ (2000). Rapid, synaptically driven increases in the intrinsic excitability of cerebellar deep nuclear neurons. *Nat Neurosci* **3**, 109–111.

Amaral D & Lavenex P (2007). Hippocampal neuroanatomy. In: *The Hippocampus Book*, ed. Andersen P, Morris R, Amaral D, Bliss TV & O'Keefe J, pp. 37–129. Oxford University Press, New York.

Bean BP (2007). The action potential in mammalian central neurons. *Nat Rev Neurosci* **8**, 451–465.

Ben-Ari Y (1985). Limbic seizure and brain damage produced by kainic acid: mechanisms and relevance to human temporal lobe epilepsy. *Neuroscience* **14**, 375–403.

Bliss TV & Collingridge GL (1993). A synaptic model of memory: long-term potentiation in the hippocampus. *Nature* **361**, 31–39.

Brown DA & Adams PR (1980). Muscarinic suppression of a novel voltage-sensitive K^+ current in a vertebrate neurone. *Nature* **283**, 673–676.

Brown JT & Randall A (2005). Gabapentin fails to alter P/Q-type Ca^{2+} channel-mediated synaptic transmission in the hippocampus in vitro. *Synapse* **55**, 262–269.

Caeser M, Brown DA, Gahwiler BH & Knopfel T (1993). Characterization of a calcium-dependent current generating a slow afterdepolarization of CA3 pyramidal cells in rat hippocampal slice cultures. *Eur J Neurosci* **5**, 560–569.

Chen K, Aradi I, Thon N, Eghbal-Ahmadi M, Baram TZ & Soltesz I (2001). Persistently modified h-channels after complex febrile seizures convert the seizure-induced enhancement of inhibition to hyperexcitability. *Nat Med* **7**, 331–337.

Chen S & Yaari Y (2008). Spike Ca^{2+} influx upmodulates the spike afterdepolarization and bursting via intracellular inhibition of KV7/M channels. *J Physiol* **586**, 1351–1363.

Coulter DA, Lo Turco JJ, Kubota M, Disterhoft JF, Moore JW & Alkon DL (1989). Classical conditioning reduces amplitude and duration of calcium-dependent afterhyperpolarization in rabbit hippocampal pyramidal cells. *J Neurophysiol* **61**, 971–981.

Dan Y & Poo MM (2006). Spike timing-dependent plasticity: from synapse to perception. *Physiol Rev* **86**, 1033–1048.

Dickson JM, Wilkinson ID, Howell SJ, Griffiths PD & Grunewald RA (2006). Idiopathic generalised epilepsy: a pilot study of memory and neuronal dysfunction in the temporal lobes, assessed by magnetic resonance spectroscopy. *J Neurol Neurosurg Psychiatry* **77**, 834–840.

Disterhoft JF, Coulter DA & Alkon DL (1986). Conditioning-specific membrane changes of rabbit hippocampal neurons measured in vitro. *Proc Natl Acad Sci U S A* **83**, 2733–2737.

Dudek SM & Bear MF (1992). Homosynaptic long-term depression in area CA1 of hippocampus and effects of N-methyl-D-aspartate receptor blockade. *Proc Natl Acad Sci U S A* **89**, 4363–4367.

Egorov AV, Hamam BN, Fransen E, Hasselmo ME & Alonso AA (2002). Graded persistent activity in entorhinal cortex neurons. *Nature* **420**, 173–178.

Fan Y, Fricker D, Brager DH, Chen X, Lu HC, Chitwood RA & Johnston D (2005). Activity-dependent decrease of excitability in rat hippocampal neurons through increases in I_h. *Nat Neurosci* **8**, 1542–1551.

Foffani G, Uzcategui YG, Gal B & Menendez de la Prida L (2007). Reduced spike-timing reliability correlates with the emergence of fast ripples in the rat epileptic hippocampus. *Neuron* **55**, 930–941.

Green JD (1964). The Hippocampus. *Physiol Rev* **44**, 561–608.

Gu N, Vervaeke K, Hu H & Storm JF (2005). Kv7/KCNQ/M and HCN/h, but not KCa2/SK channels, contribute to the somatic medium after-hyperpolarization and excitability control in CA1 hippocampal pyramidal cells. *J Physiol* **566**, 689–715.

Ireland DR, Guevremont D, Williams JM & Abraham WC (2004). Metabotropic glutamate receptor-mediated depression of the slow afterhyperpolarization is gated by tyrosine phosphatases in hippocampal CA1 pyramidal neurons. *J Neurophysiol* **92**, 2811–2819.

Jarsky T, Mady R, Kennedy B & Spruston N (2008). Distribution of bursting neurons in the CA1 region and the subiculum of the rat hippocampus. *J Comp Neurol* **506**, 535–547.

Jin Y, Kim SJ, Kim J, Worley PF & Linden DJ (2007). Long-term depression of mGluR1 signaling. *Neuron* **55**, 277–287.

Kaczorowski CC, Disterhoft J & Spruston N (2007). Stability and plasticity of intrinsic membrane properties in hippocampal CA1 pyramidal neurons: effects of internal anions. *J Physiol* **578**, 799–818.

Kandel ER & Spencer WA (1961). Electrophysiology of hippocampal neurons. II. After-potentials and repetitive firing. *J Neurophysiol* **24**, 243–259.

Korsgaard MP, Hartz BP, Brown WD, Ahring PK, Strobaek D & Mirza NR (2005). Anxiolytic effects of Maxipost (BMS-204352) and retigabine via activation of neuronal Kv7 channels. *J Pharmacol Exp Ther* **314**, 282–292.

Lei S, Pelkey KA, Topolnik L, Congar P, Lacaille JC & McBain CJ (2003). Depolarization-induced long-term depression at hippocampal mossy fiber-CA3 pyramidal neuron synapses. *J Neurosci* **23**, 9786–9795.

Main MJ, Cryan JE, Dupere JR, Cox B, Clare JJ & Burbidge SA (2000). Modulation of KCNQ2/3 potassium channels by the novel anticonvulsant retigabine. *Mol Pharmacol* **58**, 253–262.

McEchron MD, Weible AP & Disterhoft JF (2001). Aging and learning-specific changes in single-neuron activity in CA1 hippocampus during rabbit trace eyeblink conditioning. *J Neurophysiol* **86**, 1839–1857.

Mellor J, Nicoll RA & Schmitz D (2002). Mediation of hippocampal mossy fiber long-term potentiation by presynaptic I_h channels. *Science* **295**, 143–147.

Melyan Z, Lancaster B & Wheal HV (2004). Metabotropic regulation of intrinsic excitability by synaptic activation of kainate receptors. *J Neurosci* **24**, 4530–4534.

Melyan Z, Wheal HV & Lancaster B (2002). Metabotropic-mediated kainate receptor regulation of IsAHP and excitability in pyramidal cells. *Neuron* **34**, 107–114.

Metz AE, Jarsky T, Martina M & Spruston N (2005). R-type calcium channels contribute to afterdepolarization and bursting in hippocampal CA1 pyramidal neurons. *J Neurosci* **25**, 5763–5773.

Metz AE, Spruston N & Martina M (2007). Dendritic D-type potassium currents inhibit the spike afterdepolarization in rat hippocampal CA1 pyramidal neurons. *J Physiol* **581**, 175–187.

Moyer JR Jr, Thompson LT & Disterhoft JF (1996). Trace eyeblink conditioning increases CA1 excitability in a transient and learning-specific manner. *J Neurosci* **16**, 5536–5546.

Naundorf B, Wolf F & Volgushev M (2006). Unique features of action potential initiation in cortical neurons. *Nature* **440**, 1060–1063.

Rundfeldt C & Netzer R (2000). The novel anticonvulsant retigabine activates M-currents in Chinese hamster ovary-cells tranfected with human KCNQ2/3 subunits. *Neurosci Lett* **282**, 73–76.

Snow RW, Taylor CP & Dudek FE (1983). Electrophysiological and optical changes in slices of rat hippocampus during spreading depression. *J Neurophysiol* **50**, 561–572.

Somjen GG (2001). Mechanisms of spreading depression and hypoxic spreading depression-like depolarization. *Physiol Rev* **81**, 1065–1096.

Sourdet V, Russier M, Daoudal G, Ankri N & Debanne D (2003). Long-term enhancement of neuronal excitability and temporal fidelity mediated by metabotropic glutamate receptor subtype 5. *J Neurosci* **23**, 10238–10248.

Spruston N & McBain CJ (2007). Structural and functional properties of hippocampal neurons. In: *The Hippocampus Book*, ed. Andersen P, Morris R, Amaral D, Bliss TV & O'Keefe J, pp. 133–201. Oxford University Press, New York.

Storm JF (1987). Action potential repolarization and a fast after-hyperpolarization in rat hippocampal pyramidal cells. *J Physiol* **385**, 733–759.

Sugaya E, Takato M & Noda Y (1975). Neuronal and glial activity during spreading depression in cerebral cortex of cat. *J Neurophysiol* **38**, 822–841.

Tatulian L, Delmas P, Abogadie FC & Brown DA (2001). Activation of expressed KCNQ potassium currents and native neuronal M-type potassium currents by the anti-convulsant drug retigabine. *J Neurosci* **21**, 5535–5545.

Tsubokawa H, Offermanns S, Simon M & Kano M (2000). Calcium-dependent persistent facilitation of spike backpropagation in the CA1 pyramidal neurons. *J Neurosci* **20**, 4878–4884.

Urbani A & Belluzzi O (2000). Riluzole inhibits the persistent sodium current in mammalian CNS neurons. *Eur J Neurosci* **12**, 3567–3574.

Vervaeke K, Gu N, Agdestein C, Hu H & Storm JF (2006). Kv7/KCNQ/M-channels in rat glutamatergic hippocampal axons and their role in regulation of excitability and transmitter release. *J Physiol* **576**, 235–256.

Wang HS, Pan Z, Shi W, Brown BS, Wymore RS, Cohen IS, Dixon JE & McKinnon D (1998). KCNQ2 and KCNQ3 potassium channel subunits: molecular correlates of the M-channel. *Science* **282**, 1890–1893.

Wellmer J, Su H, Beck H & Yaari Y (2002). Long-lasting modification of intrinsic discharge properties in subicular neurons following status epilepticus. *Eur J Neurosci* **16**, 259–266.

Wickenden AD, Yu W, Zou A, Jegla T & Wagoner PK (2000). Retigabine, a novel anti-convulsant, enhances activation of KCNQ2/Q3 potassium channels. *Mol Pharmacol* **58**, 591–600.

Williams SR & Stuart GJ (1999). Mechanisms and consequences of action potential burst firing in rat neocortical pyramidal neurons. *J Physiol* **521**, 467–482.

Wittner L, Henze DA, Zaborszky L & Buzsaki G (2007). Three-dimensional reconstruction of the axon arbor of a CA3 pyramidal cell recorded and filled in vivo. *Brain Struct Funct* **212**, 75–83.

Wu WW, Chan CS, Surmeier DJ & Disterhoft JF (2008). Coupling of L-type Ca^{2+} channels to KV7/KCNQ channels creates a novel, activity-dependent, homeostatic intrinsic plasticity. *J Neurophysiol* **100**, 1897–1908.

Xu J, Kang N, Jiang L, Nedergaard M & Kang J (2005). Activity-dependent long-term potentiation of intrinsic excitability in hippocampal CA1 pyramidal neurons. *J Neurosci* **25**, 1750–1760.

Yue C, Remy S, Su H, Beck H & Yaari Y (2005). Proximal persistent Na^{+} channels drive spike afterdepolarizations and associated bursting in adult CA1 pyramidal cells. *J Neurosci* **25**, 9704–9720.

Yue C & Yaari Y (2004). KCNQ/M channels control spike afterdepolarization and burst generation in hippocampal neurons. *J Neurosci* **24**, 4614–4624.

Yue C & Yaari Y (2006). Axo-somatic and apical dendritic Kv7/M channels differentially regulate the intrinsic excitability of adult rat CA1 pyramidal cells. *J Neurophysiol* **95**, 3480–3495.

Zaczek R, Chorvat RJ, Saye JA, Pierdomenico ME, Maciag CM, Logue AR, Fisher BN, Rominger DH & Earl RA (1998). Two new potent neurotransmitter release enhancers, 10,10-bis(4-pyridinylmethyl)-9(10H)-anthracenone and 10, 10-bis(2-fluoro-4-pyridinylmethyl)-9(10H)-anthracenone: comparison to linopirdine. *J Pharmacol Exp Ther* **285**, 724–730.

Zhang W & Linden DJ (2003). The other side of the engram: experience-driven changes in neuronal intrinsic excitability. *Nat Rev Neurosci* **4**, 885–900.

Zhou JL, Shatskikh TN, Liu X & Holmes GL (2007). Impaired single cell firing and long-term potentiation parallels memory impairment following recurrent seizures. *Eur J Neurosci* **25**, 3667–3677.